

Rotation of planet-harboured stars

Pierre F. L. Maxted

Abstract The rotation rate of a star has important implications for the detectability, characterisation and stability of any planets that may be orbiting it. This chapter gives a brief overview of stellar rotation before describing the methods used to measure the rotation periods of planet host stars, the factors affecting the evolution of a star's rotation rate, stellar age estimates based on rotation, and an overview of the observed trends in the rotation properties of stars with planets.

Introduction

Stars with convective envelopes, which includes most stars known to harbour planets, show a variety of phenomena collectively known as magnetic activity. These include ultraviolet and X-ray emission, flares, and strong emission lines at optical wavelength, particularly $H\alpha$ and the Ca II H and K lines. All these phenomena are closely related to the rotation of the star because it is the interaction of rotation and convection that drives the generation of the complex surface magnetic field (Güdel 2004). This connection between rotation and magnetic activity has implications for the detectability of planets orbiting solar-type stars, the environment in which a planet exists, and can even lead to the destruction of a planet. Detectable stellar rotation enables the alignment of a star's rotation axis relative to the orbital plane of a planet to be measured, making it possible to study the dynamical history of a planetary system.

Pierre F. L. Maxted
Astrophysics Group, Keele University, Keele, Staffordshire, ST5 5BG, UK, e-mail: p.maxted@keele.ac.uk

Overview of stellar rotation

Here I provide a brief overview of the observed rotational properties of late-type main sequence stars, i.e. stars similar to most known planet host stars. A more general overview of stellar rotation can be found in Bouvier (2013).

It has been apparent since the earliest studies of stellar rotation that late-type stars tend to rotate much more slowly than early-type stars (Struve 1930). The rotation periods of main-sequence mid F-type stars ($T_{\text{eff}} \approx 6500 \text{ K}$, $M \approx 1.4M_{\odot}$) are typically a few days, corresponding to equatorial rotation velocities $V_{\text{rot}} \approx 20 - 40 \text{ km s}^{-1}$. The mean value of V_{rot} drops steady with spectral type to a typical value of a few km s^{-1} for G-type main-sequence stars older than about 1 Gyr (Gray 1982). The rotation period distribution becomes bimodal below mid-K spectral types with peaks near 20 and 40 days for mid M-type stars (McQuillan et al. 2014; Newton et al. 2016). The slow rotation of cool stars is a consequence of magnetic braking, i.e., angular momentum loss through a magnetised stellar wind (Weber and Davis 1967). The age dependence of stellar rotation can be studied using surveys of stellar rotation in open clusters. The behaviour at very young ages is complex (Gallet and Bouvier 2013), but by the age of the Hyades ($\sim 0.6 \text{ Gyr}$) there is a well-defined sequence of stars with $P_{\text{rot}} \approx 5 \text{ days}$ at $(B-V)=0.5$ (F7) to $P_{\text{rot}} \approx 12 \text{ days}$ at $(B-V)=1.2$ (K5) (Radick et al. 1987; Douglas et al. 2016). The rotation period then evolves approximately according to $P_{\text{rot}} \propto t^{\gamma}$ with $\gamma \approx 0.5$ (Skumanich 1972). Exceptions to this general behaviour are discussed below in relation to gyrochronology, i.e., the use of stellar rotation to estimate the age of a star.

Measuring stellar rotation

Methods used to study the rotation of stars in general are equally applicable to planet host stars. Additional information on the host star's rotation is available in transiting planet systems.

Rotational line broadening The observed line profile of a rotating star is broader than the intrinsic line profile emitted from each part of its surface because of the varying Doppler shift across the visible hemisphere of the star. The rotational broadening is directly related to $V_{\text{rot}} \sin i_{\star}$, where i_{\star} is the inclination of the star's rotation axis to the line of sight. For a star with rotation period P_{rot} and radius R , $V_{\text{rot}} \approx 50.6(R/R_{\odot})/(P/\text{days}) \text{ km s}^{-1}$. For a spherical star with no surface differential rotation, the shape of an intrinsically narrow stellar absorption line with rest wavelength λ_0 is given by

$$A(x) = \frac{\frac{2}{\pi} \sqrt{1-x^2} + \frac{\beta}{2} (1-x^2)}{1 + \frac{2}{3}\beta}, \quad (1)$$

where $x = (\lambda/\lambda_0 - 1)/(V_{\text{rot}} \sin i_*/c)$ and β is related to the linear limb-darkening coefficient u by $\beta = u/(1 - u)$ (Unsold 1955). This rotational broadening function also assumes that the limb darkening is the same at all wavelengths and that the intrinsic line profile is constant over the visible surface of the star, and neglects gravity darkening. These assumptions work well for the approximate $V_{\text{rot}} \sin i_*$ range $3 - 30 \text{ km s}^{-1}$, which covers the rotation rates for many planet host stars.

Equation (1) can be used to estimate the value of $V_{\text{rot}} \sin i_*$ for a star from the width of the absorption lines in its spectrum. This can be done directly from the full-width at half-minimum (FWHM) of individual lines in a high-resolution spectrum if the signal-to-noise is high enough ($S/N \approx 100$ or more). The position of the first zero in the Fourier transform of the line profile can be used to estimate $V_{\text{rot}} \sin i_*$ (Collins and Truax 1995). If the position of the second zero of the Fourier transform can be measured then the differential rotation of the star can be measured (Reiners and Schmitt 2002). Using individual lines to measure $V_{\text{rot}} \sin i_*$ becomes difficult if isolated lines cannot be identified or the signal-to-noise is not very high. In this case, the observed spectrum can be compared to synthetic spectra that have been convolved with the rotational broadening profile $A(x)$ to obtain an estimate of $V_{\text{rot}} \sin i_*$. The observed spectra of slowly-rotating stars with a similar spectral type to the target star can also be used as templates in this approach. More often, these rotationally-broadened spectra are used to create a calibration between $V_{\text{rot}} \sin i_*$ and some global measure of the average line width in the spectrum that can be easily calculated for large numbers of stars, e.g., the FWHM of the cross-correlation function (Weise et al. 2010).

Estimating $V_{\text{rot}} \sin i_*$ from using line broadening becomes difficult if the rotational line broadening is comparable to the intrinsic line width. The absorption lines in a stellar spectrum are broadened by various processes acting at microscopic scales in the line forming region, e.g., thermal line broadening and Zeeman splitting due to magnetic fields. The absorption lines are also broadened by turbulence in the photospheres of stars with convective atmospheres. Convection can be simulated using 3-dimensional radiation hydrodynamic models, but this is computationally expensive. For the 1-dimensional model atmospheres normally used for spectral analysis the effect of turbulence on large scales (macroturbulence) is approximated by convolving the spectrum with a Gaussian profile of width v_{mac} . Various calibrations for the parameter v_{mac} have been published. These typically give a value of $v_{\text{mac}} \approx 2 - 4 \text{ km s}^{-1}$ for the Sun with v_{mac} increasing with effective temperature up to $v_{\text{mac}} \approx 6 \text{ km s}^{-1}$ at $T_{\text{eff}} = 6500 \text{ K}$. Fig. 1 shows the effect of rotational broadening on synthetic spectra for a Sun-like star assuming $v_{\text{mac}} = 2 \text{ km s}^{-1}$ or $v_{\text{mac}} = 4 \text{ km s}^{-1}$. This illustrates how uncertainties in the intrinsic line profile of the star can lead to systematic errors 1 km s^{-1} or more in the estimates of $V_{\text{rot}} \sin i_*$ if this quantity is a few km s^{-1} or less. Similar problems can occur if $V_{\text{rot}} \sin i_*$ is less than the resolution of the spectrograph used to obtain the spectrum. Surface differential rotation can also lead to systematic errors in estimating $V_{\text{rot}} \sin i_*$ because the line profiles are the result of the integrated flux from the visible stellar surface, not just the equator. For example, Valenti and Piskunov (1996) find that $V_{\text{rot}} \sin i_* \approx 1.6 \text{ km s}^{-1}$ provides

the best match to the width of the lines in solar spectrum neglecting differential rotation, significantly lower than the true value $V_{\text{rot}} \sin i_{\star} = 2.0 \text{ km s}^{-1}$.

The precision of a radial velocity measurement from one weak absorption line can be estimated from $\sigma_v \approx \text{FWHM}^{3/2} / (W \sqrt{I_0})$, where W is the equivalent width of the line and I_0 is the signal-to-noise ratio (Beatty and Gaudi 2015). There is also additional noise in radial velocity measurements for cool stars (jitter) due to turbulence in their atmospheres and star spots, particularly for magnetically active stars (Wright 2005). This makes it easier to find planets around slowly rotating stars that have narrower spectral lines and are less magnetically active.

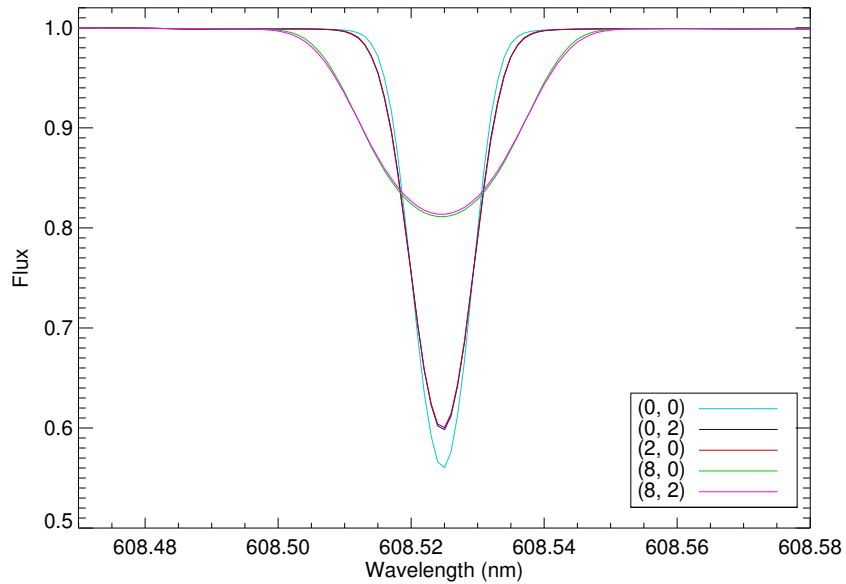


Fig. 1 Synthetic spectra in the region of an isolated Fe I line for a Sun-like star. The values of $(V_{\text{rot}} \sin i_{\star}, v_{\text{mac}})$ in km s^{-1} are noted in the legend.

Light curve modulation Total solar irradiance (TSI) varies quasi-periodically with a timescale ≈ 26 days, particularly during solar maximum (Fig. 2). This is mostly due to the changing visibility of long-lived sunspots as the Sun rotates. Similar variability is seen in the optical light curves of solar-type stars and so the timescale of these variations is interpreted as the rotation periods of these stars at the latitudes of their magnetically active regions. The timescale of the variations is normally measured using either Fourier methods (Maxted et al. 2011), from the auto-correlation function (McQuillan et al. 2013a), or using wavelet decomposition (García et al. 2014). The rotation period derived from a light curve with limited coverage can be ambiguous by a factor of two if there are two large active regions on opposite hemispheres of the star. In general, there is good agreement between the rotation periods

derived from the modulation of the flux and those obtained from the spectroscopic $V_{\text{rot}} \sin i_*$ for stars where an estimate of the radius is available.

Spot crossing events If a planet crosses a dark spot on the stellar surface during a transit there will be an anomalous “bump” in the light curve. With high quality photometry it may be possible to detect consecutive spot crossing events and so infer the rotation period of the star (Silva-Valio 2008). This method also provides useful constraints on the angle between the orbital axis of the planet and the rotation axis of the star (Tregloan-Reed et al. 2013; Béky et al. 2014).

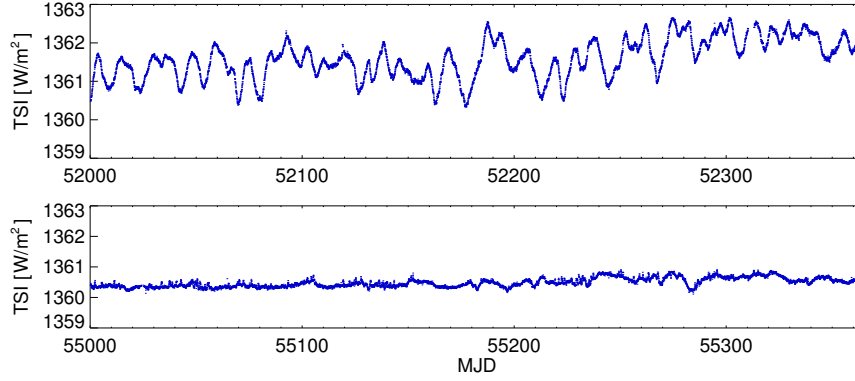


Fig. 2 Total solar irradiance (TSI) during solar maximum (upper panel) and solar minimum (lower panel) (Frölich et al. 1995). MJD is the modified Julian Date.

Asteroseismology Asteroseismology uses frequency analysis of stellar light curves to infer the interior structure, composition and other fundamental parameters of pulsating stars. Solar-type stars show variations in brightness with periods ≈ 5 minutes due to stochastic excitation of oscillation modes driven by convection. These variations are small and have a complex spectrum so extensive application of asteroseismology to solar-type stars is only possible using very high-quality photometry from instruments such as CoRoT (Auvergne et al. 2009) and Kepler (Borucki et al. 2010). The frequency of the mode with radial order n and angular degree ℓ is split into $(2\ell + 1)$ components according to the azimuthal order m . For slowly-rotating Sun-like stars this splitting is given by

$$\nu_{n,\ell,m} \approx \nu_{n,\ell} + m\Omega/2\pi, \quad (2)$$

where Ω is the average angular velocity in the outer layers of the star (Gizon et al. 2013). In addition, the amplitudes of modes with different values of m can be used to infer the inclination of the rotation axis to the line of sight. Asteroseismology can also be used to estimate the mass and age of a star by comparing its pulsation

frequencies and other observed properties to the predictions of stellar evolutionary models.

Rossiter-McLaughlin effect The transit of a star by a planet distorts the stellar absorption line profiles. With very high quality spectra it is possible to observe this distortion directly (Cegla et al. 2016), but it is more common to measure it indirectly using the mean Doppler shift of the stellar spectrum. This apparent Doppler shift shows an anomalous variation during the transit known as the Rossiter-McLaughlin (R-M) effect. The shape and amplitude of the R-M effect for a star of radius R_* orbited by a planet of radius R_p with orbital inclination i_p and semi-major axis a depend mostly on $V_{\text{rot}} \sin i_*$, the impact parameter $b = a \cos(i_p)/R_*$, $k = R_p/R_*$ and the sky-projected angle between the stellar rotation axis and the orbital angular momentum vector, λ . The line profile is asymmetric so there is also a dependence on the method used to measure the apparent Doppler shift (Hirano et al. 2011; Ohta et al. 2005; Boué et al. 2013). Doppler tomography can be used to detect the distortion to the line profile directly from an average line profile. This method works particularly well for rapidly rotating stars such as the A-type planet host WASP-33, and may be the only practical way to confirm the existence of a planetary companion to such stars (Collier Cameron et al. 2010).

Observations of the R-M effect generally focus on the derivation of λ for transiting exoplanets, but can also provide useful constraints on $V_{\text{rot}} \sin i_*$. The model degeneracies between $V_{\text{rot}} \sin i_*$ and the other model parameters are complex and can lead to implausible solutions for the least-squares fit to the R-M effect, particularly when the detection of the effect is marginal. The value of $V_{\text{rot}} \sin i_*$ derived from the line broadening can be imposed as a constraint for the analysis in these cases (Triaud et al. 2010; Albrecht et al. 2012).

Rotational evolution

The distortion of a star of mass M_1 and radius R_1 by a planet of mass M_2 at a distance d is approximately $\varepsilon = (M_2/M_1)(R_1/d)^3$, so tides are of greatest relevance to stars with massive exoplanets in close orbits, i.e., hot Jupiter systems. This distortion varies throughout the planet’s orbit unless the star’s rotation period equals the planet’s orbital period (synchronous rotation), the planet’s orbit is circular, and the orbit is aligned with the star’s rotation axis (zero obliquity). In general, the varying distortion of the star leads to dissipation of energy in the star and the exchange of angular momentum between the rotation of a star and the orbit of the planet (Ogilvie 2014). For most hot Jupiter systems the angular momentum is lost from the orbit of the planet resulting in the “spin-up” of the host star and the eventual destruction of the planet (Levrard et al. 2009; Matsumura et al. 2010). The lifetimes of hot Jupiters are directly related to the modified tidal quality factor of the star, Q'_* . Q'_* depends strongly on the properties of the star, and also depends on the frequency and amplitude of the tidal distortion itself, i.e., tidal dissipation is a non-linear problem. As a

result, it is very difficult to predict an accurate value of Q'_* for a given planetary system. Levrard et al. (2009) adopt a value $Q'_* = 10^6$ to derive lifetimes of about 1 Gyr for a typical hot Jupiter system, but stress that this parameter could be anywhere in the range $10^5 < Q'_* < 10^{10}$.

The spin-up of a star with a convective envelope by a hot Jupiter companion will lead to increased magnetic activity and, perhaps, an increase in magnetic braking. This may lead to a long-lived pseudo-stable equilibrium state for the star in which there is a balance between the angular momentum loss by magnetic braking and spin-up by a hot Jupiter companion (Dobbs-Dixon et al. 2004; Damiani and Lanza 2015). Hot Jupiters can also modify the global structure of the stellar corona and the stellar wind, reducing the efficiency of magnetic stellar wind braking (Cohen et al. 2010), i.e., hot Jupiters may prevent spin-down in some stars, as well as causing spin-up due to tidal dissipation.

The spin-up of a Sun-like star by a companion of 1 Jupiter mass is expected to be negligible if their initial separation is larger than 0.04–0.08 AU (Ferraz-Mello et al. 2015), i.e., initial periods longer than 3–8 days, where the uncertainty in this estimate is dominated by the assumed value of Q'_* . Tides are much weaker for stars with smaller radii so the spin-up of low mass stars (M-dwarfs) by planetary companions is expected to be negligible if the planet survives the initial contraction onto the main sequence (Bolmont et al. 2012). For more massive stars, tidal dissipation and magnetic braking can lead to the planet falling into the star during its main-sequence life time. Tidal dissipation also plays a role in the engulfment of planets by stars as they evolve to become red giants (Privitera et al. 2016). These merger events may be directly observable (Metzger et al. 2012) and can alter the surface composition of the star (Siess and Livio 1999), and will almost certainly result in the spin-up of the star due to the accretion of the planet’s orbital angular momentum.

Gyrochronology

The observation that older stars tend to rotate more slowly than younger stars provides a means to estimate the age of a star based on its rotation period, a technique known as gyrochronology. Barnes (2010) recommends the following equation to estimate the age (t) for a star with measured rotation period P :

$$t = \frac{\tau}{k_C} \ln \left(\frac{P}{P_0} \right) + \frac{k_I}{2\tau} (P^2 - P_0^2), \quad (3)$$

where $P_0 \approx 1.1$ d is the rotation period on the zero-age main sequence (ZAMS) and τ is the convective turnover timescale. The constants k_C and k_I have the values $k_C = 0.646$ d/Myr and $k_I = 452$ Myr/d when τ is taken from Table 1 of Barnes and Kim (2010). These values are chosen to match the rotational behaviour of stars in young open clusters ($t \approx 150$ Myr) and the rotation period of the Sun at its current age. Magnetic activity does not increase with rotation rate above some limit for

stars with very rapid rotation. The first term on the right hand side of equation (3) accounts for this saturation effect in young stars. The second term is the Skumanich-like relation, $P_{\text{rot}} \propto t^{0.5}$ that dominates for older stars. This formulation provides a better fit to the rotational behaviour of young stars than formulae that use only a Skumanich-like relation.

Until recently, the calibration of gyrochronology was based only on stars in open clusters younger than 1 Gyr plus the Sun. The Kepler mission has made it possible to test gyrochronology for stars in open clusters with ages similar to the Sun (Fig. 3). Applying equation (3) to stars observed using Kepler in NGC 6819 and M67 gives predicted ages of 2.5 Gyr with a standard deviation of 0.25 Gyr and 4.2 Gyr with a standard deviation of 0.7 Gyr, respectively. These estimates are consistent with other age estimates for stars in these clusters.

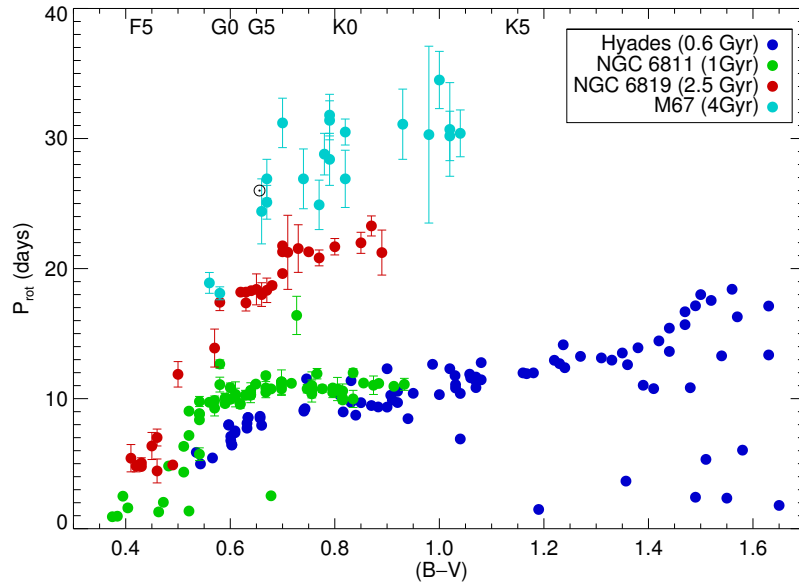


Fig. 3 Rotation periods of stars in selected open clusters and the Sun (\odot) as a function of (B–V) photometric colour (Barnes et al. 2016b; Meibom et al. 2015; Radick et al. 1987, 1995; Meibom et al. 2011).

Gyrochronology is only applicable to solar-type dwarf stars that spin-down due to magnetic braking. It is not expected to give reliable age estimates for the following types of star.

Stars in close binaries. Strong tidal interaction forces stars to rotate synchronously with the orbital period in binary systems with orbital periods ≈ 10 d or less. (Torres et al. 2010). The question of whether tidal dissipation affects gyrochronological ages for planet host stars is discussed below.

Evolved stars. The internal structure of a star and its radius both evolve rapidly when it reaches the main-sequence turn off. Barnes et al. (2016a) recommend that gyrochronology only be applied to stars with surface gravity $\log g \geq 4.3$ (where the units for g are cm s^{-2}).

Metal-poor and metal-rich stars Gyrochronology has thus far only been calibrated using open cluster data for stars close to solar metallicity. Magnetic braking may be different for stars with non-solar metallicity.

Very young stars There is considerable scatter in the rotation periods of stars on the ZAMS, from $P_0 = 0.2$ to 4.3 days. Since magnetic braking is more efficient for more rapidly rotating stars, this initial wide spread in rotation periods converges with time to about 25% by the age of the Hyades. This behaviour can be modelled approximately using equation (3) by varying P_0 , but is not included at all in prescriptions for gyrochronology that use only a Skumanich-like spin-down law. In either case, the gyrochronological ages for young stars can be very uncertain.

van Saders et al. (2016) used Kepler photometry to measure the rotation periods of 21 stars with precise ages derived using asteroseismology. They find that some stars in this sample rotate significantly faster than predicted by gyrochronology. van Saders et al interpret these observations as evidence for weakened magnetic braking in stars more evolved than the Sun. Barnes et al. (2016a) argue that this conclusion is a consequence of including evolved stars and metal-poor stars in the sample. Excluding these stars and one other from the sample, Barnes et al find that gyrochronological ages estimated using equation (3) are consistent with the age estimate from asteroseismology for the remaining eight stars to within about 12%. This is similar to the conclusion of do Nascimento et al. (2014) who applied equation (3) to 8 solar-type dwarf stars observed with Kepler with ages estimated using asteroseismology of 1–8 Gyr, although the uncertainties on the age estimates in that case were quite large (≈ 2 Gyr).

There have been other claims that gyrochronological ages may be unreliable for field stars (Angus et al. 2015; Janes 2017; Kovács 2015). All of these studies suffer from contamination of the samples studied by stars for which gyrochronology is not expected to produce reliable results and, like all surveys, will have some selection effects and biases. This is currently an active topic of debate within the scientific literature so it remains to be seen whether these issues are sufficient to explain these apparent discrepancies.

Observed trends in planet host star rotation

The three main sources of exoplanet discoveries that provide sufficient numbers for statistical analysis of the host star properties are wide area transit surveys, radial velocity surveys and the Kepler mission. We will look at the rotation properties of the planet host stars from each type of survey together since the selection effects and detection biases are broadly similar within each of these groups.

Radial velocity surveys

Surveys such as the Anglo-Australian planet search (Tinney et al. 2001), the HARPS search for southern extrasolar planets (Lo Curto et al. 2010) and the California Planet Survey (Howard et al. 2010) typically target bright G- and K-type stars that are pre-selected to have low rotation velocities and/or low levels of magnetic activity. This maximises the sensitivity of these surveys to long-period, low-mass planets, but makes it very difficult to draw conclusions about the general rotational behaviour of stars with planets from these surveys. Another complication is that the planets discovered by these surveys rarely turn out to be transiting systems. There is usually very little information available on the properties of non-transiting planets discovered in radial velocity surveys beyond a lower limit to their mass, their orbital periods, and the eccentricity of their orbits.

Comparisons between stars with and without detected planets from radial velocity surveys find that any difference in $V_{\text{rot}} \sin i_*$ between these groups is either small or not significant (Gonzalez 2011; Alves et al. 2010). Apart from the selection effects and biases in the surveys, the rotation periods of solar type stars are strongly correlated with their mass, age and metallicity. This makes it very difficult to interpret any small difference in $V_{\text{rot}} \sin i_*$ between stars with and without detected planets, particularly if these two groups come from samples with different selection effects. For example, a small difference in $V_{\text{rot}} \sin i_*$ could be due to the stars with planets being older on average than stars without detected planets, rather than due to the presence of a planet itself. The convergence of rotation periods due to magnetic braking also means that any initial difference in rotation periods between stars with and without planets will be severely reduced over the lifetime of these stars except for the small number of hot Jupiter systems found by these surveys.

Kepler objects of interest

The Kepler mission obtained high-precision photometry for almost 200,000 stars during a four year period in a 115-square-degree region of the sky with the aim of detecting transiting Earth-sized planets orbiting in the habitable zone of solar-like stars (Borucki et al. 2008; Twicken et al. 2016). Stars with Kepler data that are consistent with planetary transits are designated as Kepler objects of interest (KOIs). Fressin et al. (2013) used Kepler data from the first 18 months of the mission to show that approximately half of all stars observed by Kepler have at least one planet in the period range 0.8 – 85 days. This estimate is based on 2,222 KOIs in a sample of 156,453 stars and accounts for the fact that only about 1/40 planetary systems in this period range will show detectable transits.

McQuillan et al. (2013b) measured the rotation periods for 737 KOI using Kepler photometry for 1919 KOIs with main-sequence host stars. Their results are shown as a function of orbital period in Fig. 4. There is a noticeable dearth of planets with short orbital periods among rapidly-rotating stars. Teitler and Königl (2014)

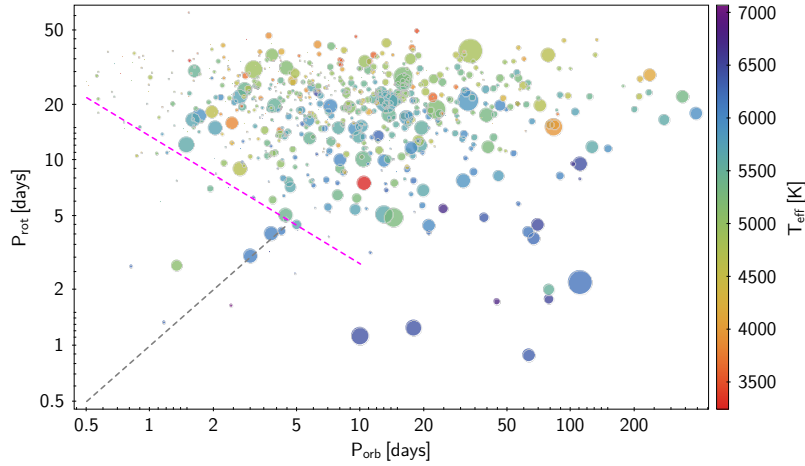


Fig. 4 Stellar rotation as a function of orbital period of the innermost planet for the 737 Kepler object interest (KOIs) from Table 1 of McQuillan et al. (2013b). Symbol size is proportional to the logarithm of the planet size. Note the lack of KOIs between the magenta dashed line and the grey dashed line that indicates $P_{\text{rot}} = P_{\text{orb}}$.

have interpreted these observations as evidence for the destruction of planets in short-period orbits in these systems, resulting in the spin-up of the host star. In this scenario, the planet responsible for the transit in these KOIs is the survivor of what was originally (and may still be) a multi-planet system. This scenario also makes the testable prediction that systems close to the limit of destruction (marked with a magenta line in Fig. 4) should, on average, be younger than systems with comparable rotation periods but longer orbital periods. These systems are currently in the process of angular momentum being transferred from the planet’s orbit to the star, so are not suitable targets for gyrochronology. Indeed, Walkowicz and Basri (2013) find some evidence that some stars with large planetary companions rotate synchronously for orbital periods $P \lesssim 10$ days, although this claim has to be treated with some caution because there is a high rate of false-positive planet detections in this part of the $P_{\text{rot}} - P_{\text{orb}}$ diagram due to contamination of the Kepler photometry by eclipsing binary stars.

Walkowicz and Basri (2013) also used published $V_{\text{rot}} \sin i_*$ measurements for a small subset of their sample together with estimates of the stellar radius to estimate i_* for these stars. They find that this method fails for rotation periods $P \gtrsim 25$ days because the rotational line broadening is too small to be measured reliably. Among the shorter period systems they find most stars are consistent with $i_* \approx 90^\circ$ if some allowance is made for systematic errors in the estimates of $V_{\text{rot}} \sin i_*$, as is expected if most transiting planets have orbits with low obliquity. One exception is Kepler-9, a star that shows transits from at least 3 planetary companions for which $i_* \approx 45^\circ$. Hirano et al. (2014) found similar results from their sample of 32 KOIs for which they measured $V_{\text{rot}} \sin i_*$, and identified three other multi-planet systems that

may have significant non-zero obliquity. These systems are useful for studying the dynamical effects that can occur during planet formation (Lai 2014; Hansen 2017).

The large number of stars that have planets that are not detected make it difficult to interpret any observed difference in the rotation periods between KOIs and non-KOIs in the Kepler sample, particularly given that there is a detection bias against planets that transit rapidly rotating solar-type stars because of additional noise from stellar activity.

Wide area surveys and hot Jupiters

KOIs are typically quite faint, with most having apparent magnitudes in the Kepler bandpass $K_p = 12 - 16$, so most planet host stars bright enough for detailed characterisation come from wide-area surveys such as WASP (Pollacco et al. 2006) and HAT (Bakos et al. 2004). The quality of the photometry achievable by these ground-based surveys restricts them to discovering planets with radii $R \gtrsim 0.5 R_{\text{Jup}}$ with orbital periods less $P \lesssim 10$ days, i.e., hot Jupiter systems. We also discuss in this sub-section results for other bright hot-Jupiter systems such as those discovered by the CoRoT mission.

Pont (2009) found tentative evidence that the host stars of some hot Jupiters rotate faster than typical stars of the same spectral type, particularly for systems where the tidal interaction between the star and the planet is large. This study was based on a sample of about 25 transiting systems with published $V_{\text{rot}} \sin i_*$ or P_{rot} estimates available at that time. Maxted et al. (2015) used Bayesian techniques to compare the age estimates from stellar model isochrones to gyrochronological age estimates for 28 transiting exoplanet host stars with accurate mass and radius estimates and directly measured rotation periods. The gyrochronological age estimate was significantly lower than the isochronal age estimate for about half of the stars in that sample. They found no clear correlation between the gyrochronological age estimate and the strength of the tidal force on the star due to the innermost planet, leading them to conclude that tidal spin-up is a reasonable explanation for this discrepancy in some cases, but not all. For example, they could find no satisfactory explanation for the discrepancy between the young age for CoRoT-2 estimated from gyrochronology and supported by its high lithium abundance, and the extremely old age for its K-type stellar companion inferred from its lack of magnetic activity. Maxted et al suggest that this may point to problems with the stellar models for some planet host stars.

References

- Albrecht S, Winn JN, Johnson JA et al. (2012) Obliquities of Hot Jupiter Host Stars: Evidence for Tidal Interactions and Primordial Misalignments. *ApJ*757:18

- Alves S, Do Nascimento JD Jr de Medeiros JR (2010) On the rotational behaviour of parent stars of extrasolar planets. *MNRAS*408:1770–1777
- Angus R, Aigrain S, Foreman-Mackey D McQuillan A (2015) Calibrating gyrochronology using Kepler asteroseismic targets. *MNRAS*450:1787–1798
- Auvergne M, Bodin P, Boisnard L et al. (2009) The CoRoT satellite in flight: description and performance. *A&A*506:411–424
- Bakos G, Noyes RW, Kovács G et al. (2004) Wide-Field Millimagnitude Photometry with the HAT: A Tool for Extrasolar Planet Detection. *PASP*116:266–277
- Barnes SA (2010) A Simple Nonlinear Model for the Rotation of Main-sequence Cool Stars. I. Introduction, Implications for Gyrochronology, and Color-Period Diagrams. *ApJ*722:222–234
- Barnes SA Kim YC (2010) Angular Momentum Loss from Cool Stars: An Empirical Expression and Connection to Stellar Activity. *ApJ*721:675
- Barnes SA, Spada F Weingrill J (2016a) Some aspects of cool main sequence star ages derived from stellar rotation (gyrochronology). *Astronomische Nachrichten* 337:810
- Barnes SA, Weingrill J, Fritzewski D, Strassmeier KG Platais I (2016b) Rotation Periods for Cool Stars in the 4 Gyr old Open Cluster M67, The Solar-Stellar Connection, and the Applicability of Gyrochronology to at least Solar Age. *ApJ*823:16
- Beatty TG Gaudi BS (2015) Astrophysical Sources of Statistical Uncertainty in Precision Radial Velocities and Their Approximations. *PASP*127:1240
- Béky B, Holman MJ, Kipping DM Noyes RW (2014) Stellar Rotation-Planetary Orbit Period Commensurability in the HAT-P-11 System. *ApJ*788:1
- Bolmont E, Raymond SN, Leconte J Matt SP (2012) Effect of the stellar spin history on the tidal evolution of close-in planets. *A&A*544:A124
- Borucki W, Koch D, Basri G et al. (2008) Finding Earth-size planets in the habitable zone: the Kepler Mission. In: Sun YS, Ferraz-Mello S Zhou JL (eds) *Exoplanets: Detection, Formation and Dynamics*, IAU Symposium, vol 249, pp 17–24, DOI 10.1017/S174392130801630X
- Borucki WJ, Koch D, Basri G et al. (2010) Kepler Planet-Detection Mission: Introduction and First Results. *Science* 327:977
- Boué G, Montalto M, Boisse I, Oshagh M Santos NC (2013) New analytical expressions of the Rossiter-McLaughlin effect adapted to different observation techniques. *A&A*550:A53
- Bouvier J (2013) Observational studies of stellar rotation. In: Hennebelle P Charbonnel C (eds) *EAS Publications Series*, *EAS Publications Series*, vol 62, pp 143–168, DOI 10.1051/eas/1362005
- Cegla HM, Lovis C, Bourrier V et al. (2016) The Rossiter-McLaughlin effect reloaded: Probing the 3D spin-orbit geometry, differential stellar rotation, and the spatially-resolved stellar spectrum of star-planet systems. *A&A*588:A127
- Cohen O, Drake JJ, Kashyap VL, Sokolov IV Gombosi TI (2010) The Impact of Hot Jupiters on the Spin-down of their Host Stars. *ApJ*723:L64–L67
- Collier Cameron A, Guenther E, Smalley B et al. (2010) Line-profile tomography of exoplanet transits - II. A gas-giant planet transiting a rapidly rotating A5 star. *MNRAS*407:507–514
- Collins GW II Truax RJ (1995) Classical rotational broadening of spectral lines. *ApJ*439:860–874
- Damiani C Lanza AF (2015) Evolution of angular-momentum-losing exoplanetary systems. Revisiting Darwin stability. *A&A*574:A39
- do Nascimento JD Jr, García RA, Mathur S et al. (2014) Rotation Periods and Ages of Solar Analogs and Solar Twins Revealed by the Kepler Mission. *ApJ*790:L23
- Dobbs-Dixon I, Lin DNC Mardling RA (2004) Spin-Orbit Evolution of Short-Period Planets. *ApJ*610:464–476
- Douglas ST, Agüeros MA, Covey KR et al. (2016) K2 Rotation Periods for Low-mass Hyads and the Implications for Gyrochronology. *ApJ*822:47
- Ferraz-Mello S, Tadeu dos Santos M, Folonier H et al. (2015) Interplay of Tidal Evolution and Stellar Wind Braking in the Rotation of Stars Hosting Massive Close-In Planets. *ApJ*807:78
- Fressin F, Torres G, Charbonneau D et al. (2013) The False Positive Rate of Kepler and the Occurrence of Planets. *ApJ*766:81

- Frölich C et al. (1995) VIRGO: Experiment for Helioseismology and Solar Irradiance Monitoring. *Sol Phys* 162:101–128
- Gallet F Bouvier J (2013) Improved angular momentum evolution model for solar-like stars. *A&A*556:A36
- García RA, Ceillier T, Salabert D et al. (2014) Rotation and magnetism of Kepler pulsating solar-like stars. Towards asteroseismically calibrated age-rotation relations. *A&A*572:A34
- Gizon L, Ballot J, Michel E et al. (2013) Seismic constraints on rotation of Sun-like star and mass of exoplanet. *Proceedings of the National Academy of Science* 110:13,267–13,271
- Gonzalez G (2011) Parent stars of extrasolar planets - XII. Additional evidence for trends with $v \sin i$, condensation temperature and chromospheric activity. *MNRAS*416:L80–L83
- Gray DF (1982) The rotation of cool main-sequence stars. *ApJ*261:259–264
- Güdel M (2004) X-ray astronomy of stellar coronae. *A&A Rev*12:71–237
- Hansen BMS (2017) Perturbation of Compact Planetary Systems by Distant Giant Planets. *MNRAS*
- Hirano T, Suto Y, Winn JN et al. (2011) Improved Modeling of the Rossiter-McLaughlin Effect for Transiting Exoplanets. *ApJ*742:69
- Hirano T, Sanchis-Ojeda R, Takeda Y et al. (2014) Measurements of Stellar Inclinations for Kepler Planet Candidates. II. Candidate Spin-Orbit Misalignments in Single- and Multiple-transiting Systems. *ApJ*783:9
- Howard AW, Johnson JA, Marcy GW et al. (2010) The California Planet Survey. I. Four New Giant Exoplanets. *ApJ*721:1467–1481
- Janes KA (2017) Rotation Periods of Wide Binaries in the Kepler Field. *ApJ*835:75
- Kovács G (2015) Are the gyro-ages of field stars underestimated? *A&A*581:A2
- Lai D (2014) Star-disc-binary interactions in protoplanetary disc systems and primordial spin-orbit misalignments. *MNRAS*440:3532–3544
- Levrard B, Winisdoerffer C Chabrier G (2009) Falling Transiting Extrasolar Giant Planets. *ApJ*692:L9–L13
- Lo Curto G, Mayor M, Benz W et al. (2010) The HARPS search for southern extra-solar planets . XXII. Multiple planet systems from the HARPS volume limited sample. *A&A*512:A48
- Matsumura S, Peale SJ Rasio FA (2010) Tidal Evolution of Close-in Planets. *ApJ*725:1995–2016
- Maxted PFL, Anderson DR, Collier Cameron A et al. (2011) WASP-41b: A Transiting Hot Jupiter Planet Orbiting a Magnetically Active G8V Star. *PASP*123:547–554
- Maxted PFL, Serenelli AM Southworth J (2015) Comparison of gyrochronological and isochronal age estimates for transiting exoplanet host stars. *A&A*577:A90
- McQuillan A, Aigrain S Mazeh T (2013a) Measuring the rotation period distribution of field M dwarfs with Kepler. *MNRAS*432:1203–1216
- McQuillan A, Mazeh T Aigrain S (2013b) Stellar Rotation Periods of the Kepler Objects of Interest: A Dearth of Close-in Planets around Fast Rotators. *ApJ*775:L11
- McQuillan A, Mazeh T Aigrain S (2014) Rotation Periods of 34,030 Kepler Main-sequence Stars: The Full Autocorrelation Sample. *ApJS*211:24
- Meibom S, Barnes SA, Latham DW et al. (2011) The Kepler Cluster Study: Stellar Rotation in NGC 6811. *ApJ*733:L9
- Meibom S, Barnes SA, Platais I et al. (2015) A spin-down clock for cool stars from observations of a 2.5-billion-year-old cluster. *Nature*517:589–591
- Metzger BD, Giannios D Spiegel DS (2012) Optical and X-ray transients from planet-star mergers. *MNRAS*425:2778–2798
- Newton ER, Irwin J, Charbonneau D et al. (2016) The Rotation and Galactic Kinematics of Mid M Dwarfs in the Solar Neighborhood. *ApJ*821:93
- Ogilvie GI (2014) Tidal Dissipation in Stars and Giant Planets. *ARA&A*52:171–210
- Ohta Y, Taruya A Suto Y (2005) The Rossiter-McLaughlin Effect and Analytic Radial Velocity Curves for Transiting Extrasolar Planetary Systems. *ApJ*622:1118–1135
- Pollacco DL, Skillen I, Collier Cameron A et al. (2006) The WASP Project and the SuperWASP Cameras. *PASP*118:1407–1418

- Pont F (2009) Empirical evidence for tidal evolution in transiting planetary systems. *MNRAS*396:1789–1796
- Privitera G, Meynet G, Eggenberger P et al. (2016) Star-planet interactions. I. Stellar rotation and planetary orbits. *A&A*591:A45
- Radick RR, Thompson DT, Lockwood GW, Duncan DK Baggett WE (1987) The activity, variability, and rotation of lower main-sequence Hyades stars. *ApJ*321:459–472
- Radick RR, Lockwood GW, Skiff BA Thompson DT (1995) A 12 Year Photometric Study of Lower Main-Sequence Hyades Stars. *ApJ*452:332
- Reiners A Schmitt JHMM (2002) On the feasibility of the detection of differential rotation in stellar absorption profiles. *A&A*384:155–162
- Siess L Livio M (1999) The accretion of brown dwarfs and planets by giant stars - II. Solar-mass stars on the red giant branch. *MNRAS*308:1133–1149
- Silva-Valio A (2008) Estimating Stellar Rotation from Starspot Detection during Planetary Transits. *ApJ*683:L179
- Skumanich A (1972) Time Scales for CA II Emission Decay, Rotational Braking, and Lithium Depletion. *ApJ*171:565
- Struve O (1930) On the axial rotation of stars. *ApJ*72
- Teitler S Königl A (2014) Why is there a Dearth of Close-in Planets around Fast-rotating Stars? *ApJ*786:139
- Tinney CG, Butler RP, Marcy GW et al. (2001) First Results from the Anglo-Australian Planet Search: A Brown Dwarf Candidate and a 51 Peg-like Planet. *ApJ*551:507–511
- Torres G, Andersen J Giménez A (2010) Accurate masses and radii of normal stars: modern results and applications. *A&A Rev*18:67–126
- Tregloan-Reed J, Southworth J Tappert C (2013) Transits and starspots in the WASP-19 planetary system. *MNRAS*428:3671–3679
- Triaud AHMJ, Collier Cameron A, Queloz D et al. (2010) Spin-orbit angle measurements for six southern transiting planets. New insights into the dynamical origins of hot Jupiters. *A&A*524:A25
- Twicken JD, Jenkins JM, Seader SE et al. (2016) Detection of Potential Transit Signals in 17 Quarters of Kepler Data: Results of the Final Kepler Mission Transiting Planet Search (DR25). *AJ*152:158
- Unsold A (1955) *Physik der Sternatmosphären, MIT besonderer Berücksichtigung der Sonne*. Springer-Verlag
- Valenti JA Piskunov N (1996) Spectroscopy made easy: A new tool for fitting observations with synthetic spectra. *A&AS*118:595–603
- van Saders JL, Ceillier T, Metcalfe TS et al. (2016) Weakened magnetic braking as the origin of anomalously rapid rotation in old field stars. *Nature*529:181–184
- Walkowicz LM Basri GS (2013) Rotation periods, variability properties and ages for Kepler exoplanet candidate host stars. *MNRAS*436:1883–1895
- Weber EJ Davis L Jr (1967) The Angular Momentum of the Solar Wind. *ApJ*148:217–227
- Weise P, Launhardt R, Setiawan J Henning T (2010) Rotational velocities of nearby young stars. *A&A*517:A88
- Wright JT (2005) Radial Velocity Jitter in Stars from the California and Carnegie Planet Search at Keck Observatory. *PASP*117:657–664